

Thermal Analysis of Micro-Heaters using the 3D-TLM method and COMSOL Multiphysics software for MEMS based Gas Sensor

Abstract. The gas sensors with Metal-Oxide (MOx) offer new opportunities for MEMS sensors due to their low congestion, high sensibility and fast answer. Microhotplate is the key component in these sensors to control the temperature of the sensing layer. In this work a meander platinum based heater has been fabricated and design. The transmission line matrix 3D-TLM method and COMSOL software are used to predict the homogeneous temperature distribution. Thus, temperatures control of hot areas of micro-heater are very important before any gas sensors and MEMS design.

Streszczenie. Czujniki gazu z tlenkiem metalu (MOx) oferują nowe możliwości dla czujników MEMS ze względu na ich niewielkie zatkanie, wysoką czułość i szybką odpowiedź. Płyta grzejna jest kluczowym elementem tych czujników do kontrolowania temperatury warstwy czujnikowej. W tej pracy wykonano i zaprojektowano meandrowy grzejnik na bazie platyny. Metoda 3D-TLM z macierzą linii transmisyjnych i oprogramowanie COMSOL są wykorzystywane do przewidywania jednorodnego rozkładu temperatury. Dlatego kontrola temperatury gorących obszarów mikropodgrzewacza jest bardzo ważna przed jakimikolwiek czujnikami gazu i projektowaniem MEMS. (Analiza termiczna mikrogrzejników metodą 3D-TLM i oprogramowaniem COMSOL Multiphysics dla czujnika gazu MEMS)

Keywords: MEMS-based gas sensors, Micro-heater, 3D-TLM, COMSOL Multiphysics, Homogeneous temperature distribution.
Słowa kluczowe: czujniki gazu oparte na MEMS, mikronagrzewnica, 3D-TLM, COMSOL Multiphysics, jednorodny rozkład temperatury.

Introduction

MEMS-based gas sensors (Micro Electro Mechanical System) have quite interesting characteristics such as high sensitivity, low cost and more and more reduced size. MOX sensors are the most predominant solid-state gas detecting devices for domestic, commercial applications and industrial safety equipment. However, the performances of such sensors are significantly influenced by their hotplates that control the temperature of the sensing layer which should be in the requisite temperature range over the heater area, so as to detect the different gases.

These sensors were developed for the first time by Taguchi [1]. Their operating principle is based on the variation of the conductivity of a metal oxide layer depending on the surrounding gas nature. Then, the structure of these sensors could be miniaturized since their manufacture is compatible with the processes used in microelectronics. This results in low cost and the possibility of integrating these sensors and the associated electronic circuits in a single component.

Many studies have focused on the design and modeling of micro-sensors like those of M. Dumitrescu et al. [2] and S.Semancik et al. [3] Which introduce a poly-Si micro-heating plate platform on the compatible SiO₂ platform and integrated on-chip circuits. M. Afridi et al. [4] designed a monolithic MEMS-based gas sensor with a poly-Si micro-heater. After, J. Cerda Belmonte et al. [5] have described fabrication process to detect O₂ and CO gases.

In 2007, Ching-Liang Dai et al. [6] designed an on-chip humidity sensor based on WO₃ nanowires and J.F. Creemer et al. [7] proposed a TiN micro-heating plate. While, G.Velmathi et al. [8] proposed various micro-heater geometries, M. Gayake, Jianhai Sun [9, 10] compared these polyimide-based micro-heater geometries in simulation by finite element method. In 2017, T. Moseley [11] presented progress in the development of semiconductor metal oxide gas sensor technology and Qi Liu et al. [12] reviews the thermal performance possibility of micro hotplates with novel shapes based on single-layer SiO₂ suspended film. R. Jagdeep et al [13] mentioned that

there is a non-linear relationship between the voltage and the temperature generated by the heating element.

D.Berndt, et al [14] studied a thermal conductivity sensor for hydrogen gas detection where a heated filament is exposed by a selective wet etching process creating a micro-hotplate on a thin membrane. This sensor is operated in pulsed mode to minimize power consumption.

Temperature is an important factor for MOX gas sensors since it allows to catalyze the physico-chemical reactions between the sensitive layer and the detected target gas. So, the main task of micro-heater is to provide temperature uniformity (with attaining constant high temperature) for sensing layer. In addition, it must operate at less applied voltage in order to lower the power consumption and extend the sensor life.

A MEMS hotplate consisting of a double spiral platinum-based element was fabricated, designed and simulated using the three-dimensional transmission line matrix (3D-TLM) method to predict the homogeneous behavior of the temperature distribution according to the selected geometry. The TLM method has already been used successfully to model the thermal behavior of various devices [15, 16]. 3D-TLM method seems to be efficient for study thermal effects in microsystems [17].

In this work, we wrote our own software based on the TLM technique to analysis distribution of the temperature in the active zone of the gas sensor. To compare results, the COMSOLTM, commercial finite element analysis FEA software is conducted to obtain a accurate temperature distribution.

Thermal mathematical modeling of micro-heater

Transmission-Line-Matrix (TLM) method, originally used as a numerical technique for modeling electromagnetic wave propagation [18], has since been established as a powerful technique to study heat transfer, Self-heating problems, vibration, , electromagnetic compatibility, etc. The TLM method directly models a physical process because it is inherently a discrete approach. The TLM is based on the telegrapher's equation for a transmission line [19]:

$$(1) \quad \nabla^2 \Phi = A R_d C_d \frac{\partial \Phi}{\partial t} + B L_d C_d \frac{\partial \Phi}{\partial t^2}$$

where Φ is the potential, R_d , C_d and L_d are distributed resistance, capacitance and inductance, and A and B are dimension constants. If the first time derivative term on the right-hand side of (1) dominates the second term, the network models the diffusion equation described by the known equation:

$$(2) \quad \nabla^2 T = \left(\frac{\rho C_p}{K_T} \right) \cdot \frac{\partial T}{\partial t}$$

where T is the temperature, C_p is the specific heat, ρ is the density and K_T is the thermal conductivity. Therefore, the material can be replaced by a lumped RLC or transmission-lines network where temperature will be represented by voltage.

In TLM network, each node represents the material's thermal resistance by resistors grouped around the node while the capacitor/inductor elements are replaced by a loss-free transmission-line of impedance Z , which connects each node to its neighbors and moves the voltage pulses between nodes in a finite time Δt , Fig. 1.

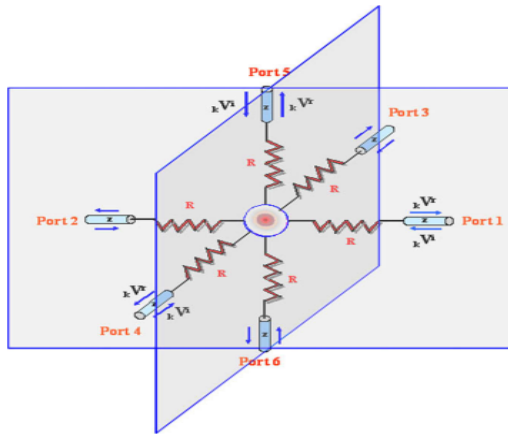


Fig.1. TLM 3D Single volume node

In fundamental transmission line theory [5], the impedance is related to C and L by:

$$(3) \quad Z = \sqrt{\frac{L}{C}} = \frac{3 \cdot \Delta t}{c} = \frac{L}{3 \cdot \Delta t}$$

Where the values of three dimensional R and a common C at each node are defined by:

$$(4) \quad R_x = \frac{\Delta x}{2 \cdot K_T \cdot \Delta y \cdot \Delta z}, \quad R_y = \frac{\Delta y}{2 \cdot K_T \cdot \Delta x \cdot \Delta z}, \quad R_z = \frac{\Delta z}{2 \cdot K_T \cdot \Delta x \cdot \Delta y}$$

$$(5) \quad C = \rho \cdot C_p \cdot \Delta x \cdot \Delta y \cdot \Delta z$$

As we have a cubic elemental volume, the three local distances between nodes are equidistant, that means; $\Delta x = \Delta y = \Delta z$. The TLM is an iterative method. Injection of delta temperature pulses is to be incident simultaneously after each time step Δt on all parts of all nodes of the network. During Δt , the incident temperature pulses are scattered instantaneously into reflected pulses which travel along link transmission and become a new incidents upon neighboring nodes. We can note that in the network, a TLM routine operates on the traveling, scattering and connecting of these thermal pulses [17].

From TLM modeling [15] the temperature at each node is given by:

$$(6) \quad {}_k T(n) = \left[\frac{2({}_k T_1^i + {}_k T_2^i)}{R_x + Z} + \frac{2({}_k T_3^i + {}_k T_4^i)}{R_y + Z} + \frac{2({}_k T_5^i + {}_k T_6^i)}{R_z + Z} \right] \cdot \frac{1}{Y}$$

Where $Y = \frac{2}{R_x + Z} + \frac{2}{R_y + Z} + \frac{2}{R_z + Z}$ and ${}_k T_j^i$ are incident pulses at the K^{ieme} iteration. Reflected pulses are calculated according to:

$$(7) \quad \begin{aligned} {}_k T_{1,2}^r(x, y, z) &= \frac{1}{R_x + Z} [Z {}_k T(x, y, z) + (R_x - Z) {}_k T_{1,2}^i(x, y, z)] \\ {}_k T_{3,4}^r(x, y, z) &= \frac{1}{R_y + Z} [Z {}_k T(x, y, z) + (R_y - Z) {}_k T_{3,4}^i(x, y, z)] \\ {}_k T_{5,6}^r(x, y, z) &= \frac{1}{R_z + Z} [Z {}_k T(x, y, z) + (R_z - Z) {}_k T_{5,6}^i(x, y, z)] \end{aligned}$$

These pulses travel to adjacent nodes to become, at the $(k+1)$ iteration, incident pulses:

$$(8) \quad {}_{k+1} T_j^i(x, y, z) = \Gamma_j(x, y, z) {}_k T_j^r(x, y, z) + [1 - \Gamma_j(u, v, w)] {}_k T_{j'}^r(u, v, w)$$

where (x, y, z) are node N co-ordinate. The reflection coefficient in direction Γ_j at concerned node is:

$$(9) \quad \Gamma_j(x, y, z) = \frac{Z(u, v, w) - Z(x, y, z)}{Z(u, v, w) + Z(x, y, z)}$$

Where, the corresponding values of the directions j, j' , and positions u, v, w are mentioned in the following Table.1.

Table.1 Corresponding values of j, j', u, v, w . [17].

j	j'	u	v	w
1	2	$x-1$	y	z
2	1	$x+1$	y	z
3	4	x	$y-1$	z
4	3	x	$y+1$	z
5	6	x	y	$z-1$
6	5	x	y	$z+1$

Implementation of a TLM routine consists solely of repeated application of equation (5) to (10). As argued by Kronberg [20], boundary conditions express the interaction of the system at hand with its surroundings. Boundaries are part of the transport model and thus should be consistent with the description of the heat transport inside the medium.

The thermal analysis provides an estimate of the temperature distribution on the plane of the heater depending on its geometrical and material parameters. Indeed, the temperature increases due to the resistive heat generated Q which is proportional to the square of the current density electric J [21]:

$$(10) \quad Q \propto |J|^2$$

The proportionality coefficient is the electrical resistivity which is also the inverse of its electrical conductivity. The current density is proportional to the electric field, which is equal to the negative of the potential gradient V . Thus, we have the following relationship:

$$(11) \quad Q = \frac{1}{\sigma} |J|^2 = \frac{1}{\sigma} |\sigma E|^2 = \sigma |\nabla V|^2$$

Where the electrical conductivity σ is expressed as:

$$(12) \quad \sigma = \frac{\sigma_0}{1 + \alpha (T - T_0)}$$

where σ_0 is the conductivity at the reference temperature T_0 . α is the temperature coefficient of resistivity. Additionally, power consumption is described as:

$$(13) \quad P = \frac{V^2}{R}$$

Where V is voltage and R stands for resistance of heating electrode. The equations have been solved under Dirichlet, Neumann, and mixed boundary conditions numerically using the Finite Element Method (FEM) selected in COMSOL.

Simulation models and results

A micro-heater should have high temperature to desired level with low power consumption. The heating of the platform is based on the joule effect by the supply of a heater. This power supply induces a flow of current in the heater causing its heating. The model related materials properties is shown in Table.2 [21,22].

Table.2 Material properties used in the thermal analysis [21].

Material	Density ρ (Kg/m ³)	Heat capacity C_p (J/Kg.K ^o)	Thermal conductivity k (W/m.K ^o)	Electric resistivity σ (Ω .m)
Si	2330	867	45.82	$3 \cdot 10^9$
SiO ₂	2220	1040	1.75	$1 \cdot 10^{13}$
Poly-Si	3280	700	180	$1.5 \cdot 10^{-0.5}$
Pt	21440	141	73.2	$3.4 \cdot 10^{-0.7}$

The model presented comprises several layers such as the platinum micro platform, silicon oxide (SiO₂) membrane with a thickness of 3 μ m and a surface area of 80 x 100 mm² used as thermal insulation. The structure of the model is

presented in Fig. 2 and the realized experimental model of the sensor in Fig.3.

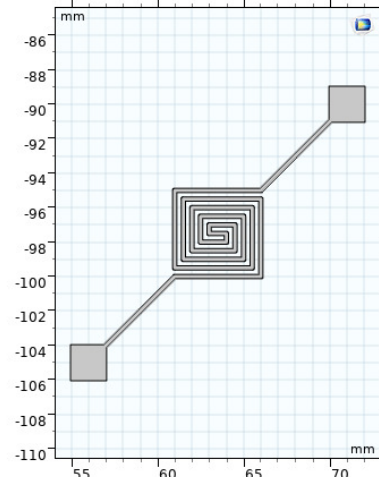


Fig.2. Micro-hotplate structure with a platinum heater

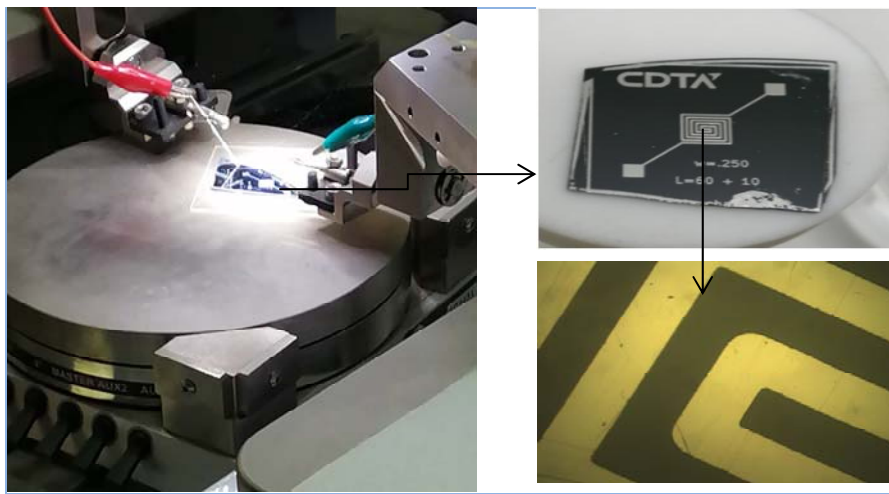


Fig.3. Presentation of the realized experimental model of the sensor

In the literature, different geometries of the heating platform are used to achieve temperature uniformity but the meander is the selected geometric shape that is intended to increase the length of the resistance to compensate for the low resistivity of the metal.

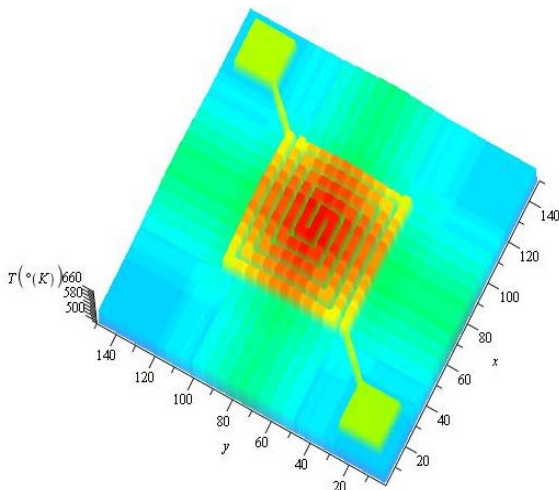


Fig.4. The thermal profile simulated by TLM method

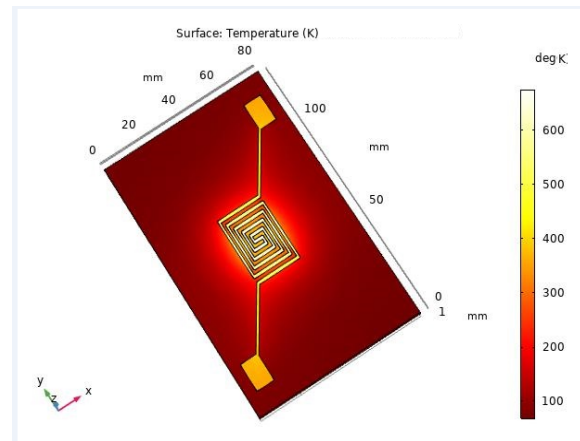


Fig.5. The thermal profile simulated by COMSOL

The distribution of the surface temperature is shown in Fig.4. The hot-area with maximum temperature which is equal approximately to 659.31 $^{\circ}$ K. Hence, the results of simulation obtained made it possible to retain that the geometry of spiral form make it possible to obtain a good thermal uniformity. The rise in temperatures easily reaches

650 °K to 660 °K for a 3V heater contact power supply. The temperature is very high since the effect of the membrane and the substrate in the diffusion of the generated heat has not been inserted in simulation. Indeed, the heating element is a key component of the sensor because it is a resistor whose role is to make after detection the S_nO_2 layer at its operating temperature. The thermal profile simulated by COMSOL, commercial finite element analysis FEA software is shown in Fig.5 with 658.52°K as maximum temperature. We can also observe a good thermal uniformity of distribution of the temperature in the active zone of the sensor.

The presentation of isothermal heat diffusion contours is illustrated in Fig.6.

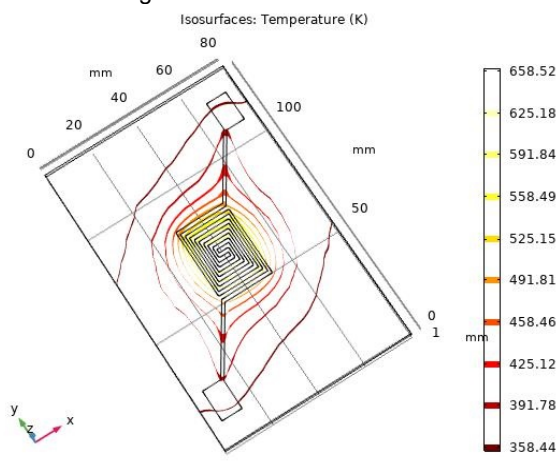


Fig.6. Presentation of isothermal heat diffusion contours

The total displacement on the membrane caused by the heat is 50 μm at the maximum operating voltage however at the sensing temperature is 20 μm (Fig. 7).

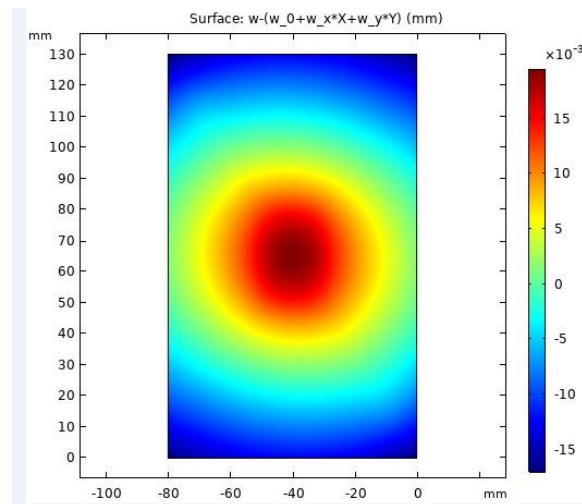


Fig.7. Presentation of 2D membrane displacement

We notice hot spots that can reach at least 30°K more than the average value of the track when the heater is brought to temperatures above 500°K, Fig.8. These localized and accentuated hot spots at the corners of the heater are a source of degradation and therefore of its drift over time. In addition, these temperatures differences may be locally modify the thermal distribution of the sensitive layer.

The Figure.9 shows comparaison between the temperature distribution along the x-axis using the TLM model and the multiphysics FEM simulation for the spiral-shaped form of micro-heater. This comparison is made at a

point of the center of the surface, where the temperature is highest.

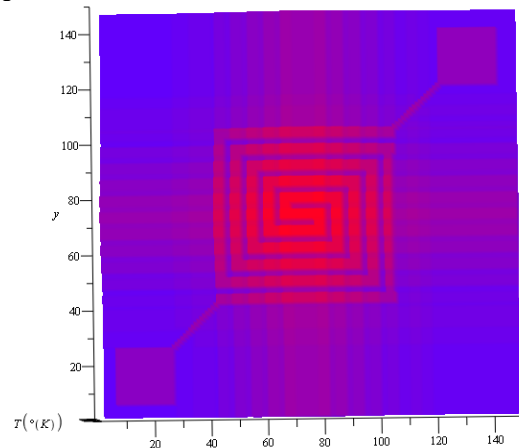


Fig.8. The temperature distributions simulated by TLM method for micro-heater

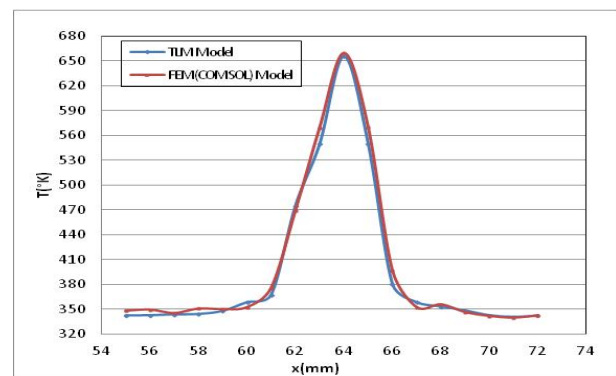


Fig.9. Comparison between 3D-TLM and multiphysics FEM simulation

The reasonable agreement between COMSOL, commercial finite element analysis FEA software and TLM-3D simulation is achieved, by accepting an error less than 2.4%. These methods can be beneficial in pre-design phase for the fast detection a large number of gases. Therefore, temperature control and the form of hot areas of micro-heater are very important in the selection of appropriate materials in any models of proposed sensors

CONCLUSION

The thermal analysis allowed simulating the operation of the heating platform of the MEMS gas sensor. This system must provide a maximum amount of heat for minimum power, while ensuring the best homogeneity of heat propagation.

A MEMS heating plate consisting of a double-spiral platinum-based element was fabricated, designed and simulated using the three-dimensional transmission line matrix (3D-TLM) method and the COMSOL Multiphysics software. In this work, we wrote our own software based on the TLM technique to analysis distribution of the temperature in the active zone of the gas sensor. To compare results, the COMSOLTM, commercial finite element analysis FEA software is conducted to obtain a accurate temperature distribution.

Good agreement is observed, with the maximum deviation between them around 2.4%. The temperature profile peaks sharply around the micro-heater's centers, indicating the homogeneous behavior of the temperature distribution according to the selected geometry of the micro-

heater. It has been noticed that localized and accentuated hot spots at the corners of the radiator reaching 30°K more than the average value of the track when the heater exceeds temperatures above 500°K. Beyond that, we can indicate that these hot spots will be a source of degradation over time and may locally modify the thermal distribution of the sensitive layer. Therefore, temperatures control and the forms of hot areas of micro-heater are very important before any gas sensors and other micro systems design.

Acknowledgments

The authors also would declare that the experimentations were done in the CDTA (Center for Development of Advanced Technologies) Baba Hassen, Alger, Algeria

The work is carried out in the Automation, Vision and Control of Industrial Systems (AVCSI) laboratory.

Authors: PhD student Kheris Djameleddine, University of USTO-Oran, department of automatic, E-mail: djameleddine.kheris@univ-usto.dz or djamelgp2@gmail.com; Prof HOCINE Rachida, Department of Automatics Engineering, University of Sciences and Technology of Oran, Algeria, E-mail: rachida.hocine@univ-usto.dz or rak-hocine@yahoo.fr.

REFERENCES

- [1] Duffie J. A. and Beckman W. A. (1991). Solar Engineering of Thermal Processes, 2nd edition, John Wiley & Sons, New York.
- [2] M. Dumitrescu, C.Cobianu, D.Dascalu, A. Pascu, S.Kolev and A.Berg (1998). Thermal simulation of surface Micromachined polysilicon hotplates of low power consumption. IEEE, pp. 83-86.
- [3] S. Semancik, R.E. Cavicchi, M.C. Wheeler, J.E. Tiffani, G.E. Poerier, R.M. Walton, J.S. Suehle, B. Panchapakesan and D.L. De Voe (2001). Microhotplate platforms for chemical sensor research. Sensors and Actuators B, vol. 77, pp. 579–591.
- [4] M. Afridi, A. Hefner, D. Berning, C. Ellenwood, A. Varma, B. Jacob and S. Semancik (2004). MEMS-based embedded sensor virtual components for system-on-a-chip (SoC). Solid-State Electronics, vol. 48, pp. 1777–1781, 2004.
- [5] J. Cerdà Belmonte, J. Puigcorbe, J. Arbiol, A.Vila, J. R. Morante, N. Sabate, I. Gracia and C. Cane. (2006). High-temperature low-power performing micro machined suspended micro-hotplate for gas sensing applications. Sensors and Actuators B, vol. 114, pp. 826–835.
- [6] Ching-Liang Dai, Mao-Chen Liu, Fu-Song Chen, Chyan-Chyi Wu and Ming-Wei Chang. (2007). A nanowire WO₃ humidity sensor integrated with micro-heater and inverting amplifier circuit on chip manufactured using CMOS-MEMS technique. Sensors and Actuators B, vol. 123, pp. 896–901.
- [7] J. F. Creemer, D. Briand, H. W. Zandbergen, W. van der Vlist, C. R. de Boer, N. F. de Rooij and P. M. Sarro. (2008). Micro hotplates with TiN heaters. Sensors and Actuators A, vol. 148, pp. 416–421.
- [8] G. Velmathi, N. Ramshanker and S. Mohan. (2010). 2D Simulations and Electro-Thermal Analysis of Micro-Heater Designs Using COMSOLTM for Gas Sensor Applications. Proceedings of the COMSOL Conference, India.
- [9] M. Gayake, D. Bokdas and S. Gangal. (2011). Simulations of Polymer based Micro-heater Operated at Low Voltage. Proceedings of the COMSOL Conference, Bangalore, India.
- [10] Jianhai Sun, Dafu Cui, L.Xing Chen, Haoyuan Cai and Hui Li. (2013). Fabrication and characterization of a double-heater based MEMS thermal flow sensor. Sensors and Actuators A, vol. 193, pp. 25– 29.
- [11] <https://iopscience.iop.org/article/10.1088/1361-6501/aa7443/meta>
- [12] Qi Liu, Guifu Ding, Yipin Wang and Jinyuan Yao. (2018). Thermal Performance of Micro Hotplates with Novel Shapes Based on Single-Layer SiO₂Suspended Film. Micro-machines, 9, 514.
- [13] Jagdeep Rahul and Kurmendra. (2019). Analysis of MEMS based Micro-hot Plate for Gas Sensor. Journal of Semiconductor Devices and Circuits ISSN: 2455-3379 (Online) Volume 6, Issue 2 www.stmjournals.com
- [14] D.Berndt, J.Muggli and F.Wittwer. (2020). " MEMS-based thermal conductivity sensor for hydrogen gas detection in automotive applications" ,Sensors and Actuators A: Physical Elsevier, Volume 305,
- [15] R. Hocine, S.H.Pulko, A. Boudghene Stambouli, A. Saidane. (2009).TLM Method for Thermal Investigation of IGBT Modules in PWM Mode. Microelectronic Engineering Journal, Elsevier Science, pp. 2053–2062.
- [16]Elkalsh, A. Vukovic, P. D. Sewell, and T. M. Benson. (2016). Electro-thermal modelling for plasmonic structures in the TLM method. Optical and Quantum Electronics, vol. 48, no. 4, p. 263.
- [17]K. Belkacemi, R.Hocine. (2018). Efficient 3D-TLM Modeling and Simulation for the Thermal Management of Microwave AlGaIn/GaN HEMT Used in High Power Amplifiers SSPA. Journal of Low Power Electronics and Applications MDPI, 8.
- [18]C. Christopoulos. (2006). "The Transmission-Line Modeling (TLM) Method in Electromagnetics", Synthesis Lectures on Computational Electromagnetics.
- [19]P.W.Webb and I. A. D. Russell. (1995). " Application of the TLM Method to Transient Thermal Simulation of Microwave Power Transistors ", IEEE Transactions on Electron Devices, Vol.42, N°4, 1995.
- [20]E.Kronberg, A.H Benneker. (1998). Notes on wave theory in heat conduction: A new boundary condition, International journal Heat Mass Transfer, Elsevier Science Ltd. Vol. 41, N°. 1 pp. 127-137. [http://dx.doi.org/10.1016/s0017-9310\(97\)00099-9](http://dx.doi.org/10.1016/s0017-9310(97)00099-9).
- [21] R.Hocine, D.Kheris et A.Benemara. (2019)." Thermal Analysis of Micro-heater using Multiphysics FEM and TLM simulations for MEMS based Gas Sensor". 5th International Conference On Advances In Mechanical Engineering Istanbul.
- [22]F. Samaeifar H. Hajghassem, A. Hassan Abdollahi. (2015). Implementation of high-performance MEMS platinum micro-hotplate. Sensor Review, Vol. 35 Issue 1 pp. - <http://dx.doi.org/10.1108/SR-05-2014-654>.